KERNFORSCHUNGSZENTRUM

KARLSRUHE

November 1970

KFK 1334

Institut für Neutronenphysik und Reaktortechnik

Calculation of Flux Distributions in Reactor Sub-Regions with Generalized Multiple Collision Probabilities

L. Mayer

GESELLSCHAFT FÜR KERNFORSCHUNG M. B. H.

KARLSRUHE

Journal of Nuclear Energy, Vol. 24, pp. 337 to 358. Pergamon Press 1970. Printed in Northern Ireland

CALCULATION OF FLUX DISTRIBUTIONS IN REACTOR SUB-REGIONS WITH GENERALIZED MULTIPLE COLLISION PROBABILITIES

L. MAYER
Kernforschungszentrum Karlsruhe, INR, 7501 Leopoldshafen, Germany

(*Received* 23 *February* 1970)

Abstract—The theory of multiple collision probabilities for one-dimensional problems has been extended for handling thick zones and strongly anisotropic fluxes. This entails the treatment of space dependent scattering sources and anisotropic fluxes at the boundaries of sub-zones. For plane geometry anisotropic scattering sources have been included. A multigroup collision probability code STOWA based on the extended theory has been written. It may be used in connection with diffusion calculations or independently and may perform cell calculations or determine flux distributions in special layers of a reactor, e.g. in the blanket or the shielding. Results are given and compared to other transport codes and measurements. Different approximations to angular scattering on hydrogen are evaluated with the code.

1. INTRODUCTION

COLLISION probabilities are commonly used for reactor cell calculations, but up to now they have not been applied to the solution of other transport problems such as the determination of the flux distribution in the outer layers of a reactor. This paper presents the derivation of generalized multiple collision probabilities suitable for the solution of a variety of one dimensional problems. With the help of a newly developed code using these collision probabilities it is tried to estimate the possibilities and the limits of multiple collision probabilities.

There are two assumptions which are commonly used in connection with multiple and first collision probabilities severely hampering the application to problems other than cell calculations. These are the flat scattering source approximation, which is valid only in narrow or suitably subdivided layers, and the cosine distribution for the neutron currents at the boundaries, which is not sufficient in regions far away from sources. In order to achieve greater flexibility in the application of the technique these approximations have been discarded in favour of the following ones:

1. The angular distribution of the current at the boundaries in each half space is approximated by a series in powers of cos α, α being the angle between neutron direction and the normal on the boundary. This is equivalent to a DP_N-approximation.
2. The scattering source distribution is approximated by a polynomial of low degree in the space variable.

Both generalizations are carried out for plane, cylindrical, and spherical geometry with a multigroup approximation for the energy dependence. An equally comprehensive generalization of multiple collision probabilities has not been undertaken up to now, though for some special cases extensions of the original formulation are to be found in literature, e.g. by AMOUYAL, BENOIST and HOROWITZ (1957); GAST (1962); SAHNI (1966); SYROS (1966) and (1967); KIER (1966) and (1967); MURLEY and KAPLAN (1967); HÖRTNER and PUTZ (1968). The scattering is assumed to be isotropic in cylindrical and spherical geometry. In plane geometry the angular dependence of the scattering

cross section can be approximated by a P_N-series, but only for neutrons remaining in the same group after scattering; downscattering is treated as isotropic in cell geometries.

The derivation of the formulas for multiple collision probabilities with the above approximations will be presented in the sections 2–5 together with the formalism for the solution of multigroup, multilayer problems. Section 6 shows the results of various calculations compared to other transport codes and measurements. In section 7 the P_N-approximation to angular scattering is used for an evaluation of different approximations to the angular dependence of scattering on hydrogen. Section 8 gives a final evaluation of the advantages and disadvantages of the method.

2. TRANSMISSION PROBABILITIES FOR ANISOTROPIC BOUNDARY FLUXES AND SPACE DEPENDENT ISOTROPIC SCATTERING SOURCES IN ALL ONE-DIMENSIONAL GEOMETRIES

The theory of multiple collision probabilities, especially its derivation from transport theory, can be found elsewhere (MÜLLER and LINNARTZ, 1963; MAYER, 1968),

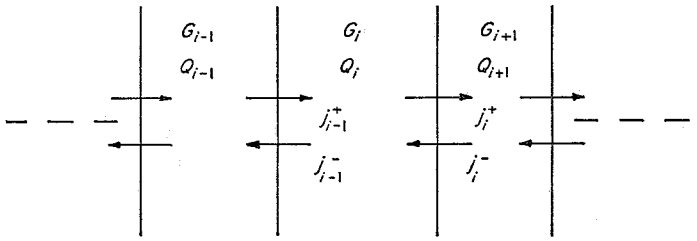

FIG. 1.—Definition of layers and partial currents.

and will not be presented in detail here. If, in the onedimensional case, the region in which the neutron fluxes shall be determined is subdivided into zones G_i according to Fig. 1, with partial neutron currents j_i^+ and j_i^- across the boundaries, the equations linking the in- and outgoing currents in zone G_i are

$$\begin{aligned} J_{i-1}^- &= S_i^{2-} J_i^- + S_i^{+-} j_{i-1}^+ + R_i^- \\ J_i^+ &= S_i^{-+} J_i^- + S_i^{2+} J_{i-1}^+ + R_i^+. \end{aligned} \tag{1}$$

Here, S_i^{2-}, S_i^{+-}, S_i^{-+} and S_i^{2+} are the transmission and reflection coefficients of G_i, and R_i^- and R_i^+ take into account the contribution of a neutron source Q_i in G_i. In the multigroup case and/or in the case of an expansion of the partial current, j_i^+ and j_i^- are vectors of the multigroup currents and/or expansion coefficients, S_i^{2-} etc. are transmission and reflection matrices, and R_i^-, R_i^+ are vectors. S_i^{2+} etc. and R_i^+, R_i^- will be determined with the multiple collision probability technique. Equations (1) together with the proper boundary conditions yield a system of equations for the partial currents which in their turn, by use of a simple neutron balance equation, serve to determine the mean fluxes in G_i. In the following, the index i indicating the different zones will be omitted for simplicity.

By following the ingoing neutrons through their successive collisions until they are either absorbed or scattered out of G, the transmission and reflections coefficients S and R are reduced to the transmission probabilities—without collision—for ingoing

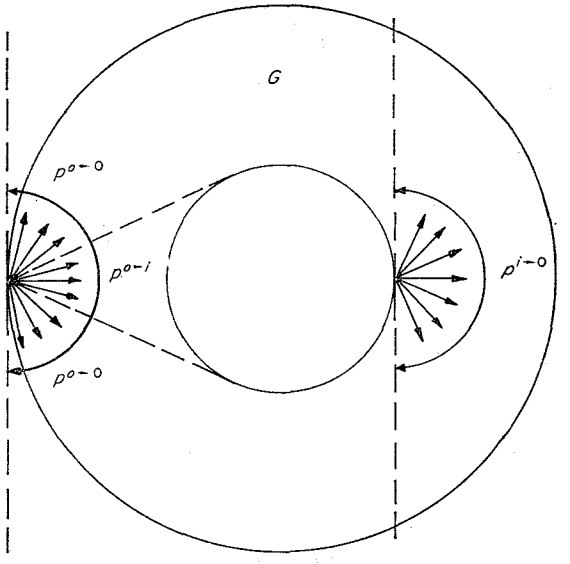

FIG. 2.—Transmission probabilities for cylindrical geometry.

currents and for scattering sources. For example in the monoenergetic case

$$S^{2+} = P_0 + (1 - P_0)\frac{\sum_s}{\sum}(P_1^+ + (1 - P_1^+ - P_1^-)\frac{\sum_s}{\sum}(P_2 + \ldots)) \qquad (2)$$

with

P_0 probability for ingoing neutrons from the left boundary to leave G_i without collision;

P_s^+ probability for neutrons scattered s times to leave G_i over the right boundary without further collision;

P_s^- same as P_s^+ for the left boundary;

$\sum_s$ scattering cross section;

$\sum$ total cross section.

Similar formulas hold for S^{-+} etc. and R^+, R^-.

The exact calculation of P_0, P_s^+, P_s^- is subject to the difficulties inherent in every transport calculation. Thus, P_0 is dependent on the angular distribution of j^+, P_1^+ and P_1^- depend on the angular and spatial distribution of the neutrons after their first collision etc.

In the following, the transmission probabilities (for transmission without collision) will be denoted by $P^{o\to i}, P^{o\to o}, P^{i\to o}, P^{v\to i}$ and $P^{v\to o}$, with o signifying the outer, i the inner boundary and v the volume—in connection with volume sources—of G (Fig. 2). The first step is to calculate the transmission probabilities $P^{o\to i}$, $P^{i\to o}$ and $P^{o\to o}$ for anisotropic flux densities at the boundaries. The angular distribution of the neutron currents at the boundaries is approximated by

$$j^{\pm}(\alpha) = \sum_{i=1}^{I} j_i^{\pm} \cos^i \alpha$$

where α is the angle between the neutron direction and the normal on the boundary. The transmission probabilities are calculated separately for each component i. As the outgoing fluxes must be represented in the same manner as the ingoing ones, one has to evaluate not only the probabilities but their first I-1 moments as well.

The technique for deriving transmission probabilities may be found in detail in the works of MÜLLER and LINNARTZ (1963) or MAYER (1968). Thus, it is sufficient to give a list of the formulas resulting for different geometries (Appendix 1).

The second step consists of the determination of the transmission probabilities for the scattering sources Q. They are approximated by

$$Q(r) = \sum_{l=0}^{L} g_l f_l(r) \tag{3}$$

with

$f_l(x) = x^l$ for plane geometry
$f_l(r) = (r^2 - k^2)^l$ for cylindrical and spherical geometry

$r = R/R_0$ is a reduced radius, $k = R_i/R_0$ the quotient of inner and outer radius. Note that for k approximately 1 with $r = k + x$, $x \ll k$:

$$f_l(r) = (2kx + x^2)^l \approx (2k)^l x^l \sim f_l(x). \tag{4}$$

Equation (4) entails a steady transition of the probabilities for spherical and cylindrical geometry into those for plane geometry with the same l. On the one hand, this makes possible an interpolation in the k-direction. On the other hand, if one chooses $f_l(r) = r^{2l}$, the limit for all values of l is $f_0(x)$. This then means a bad description of the space dependence in the case of faintly curved layers.

The transmission probabilities $P_{ij}^{v\to i}$ and $P_{ij}^{v\to 0}$ are evaluated separately for each l and each moment j and can be found in Appendix 1 for all geometries.

From these probabilities, the transmission probability for $Q(r)$ given by (3) is derived by the use of

$$P_{Q,j}^{v\to o/i} = \frac{\sum_{l=0}^{L} g_l G_l P_{l,j}^{v\to o/i}}{\sum_{l=0}^{L} g_l G_l} \tag{5}$$

with

$G_l = \dfrac{1}{l+1}$ (plane geometry)

$G_l = \dfrac{(1+k^2)^l}{l+1}$ (cylindrical geometry)

$G_l = (N_l)^{-1}$ (spherical geometry; for N_l see Appendix 1).

For the application of (5) the space dependence of the scattering source must be known. As it is represented only approximately, a few data on its exact distribution are sufficient. For neutrons scattered s times, these data are given by the transmission probabilities of the $s - 1$ times scattered neutrons. For example, $1 - P^{\to o} - P^{\to i}$ is proportional to the integrated source, while $P^{\to o}$ and $P^{\to i}$ are proportional to the source value at the outer and inner boundary. The exact relations are given in Appendix 1.

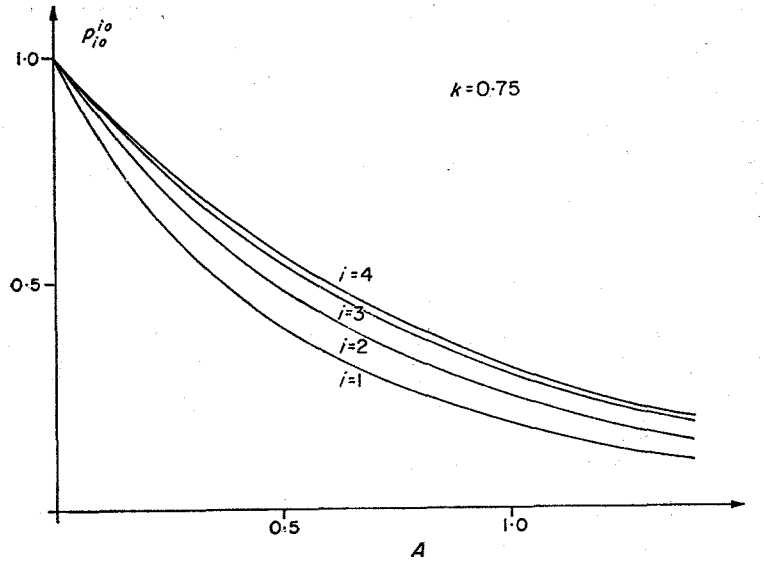

FIG. 3.—Transmission probabilities for a current $j \sim \cos^i \alpha$

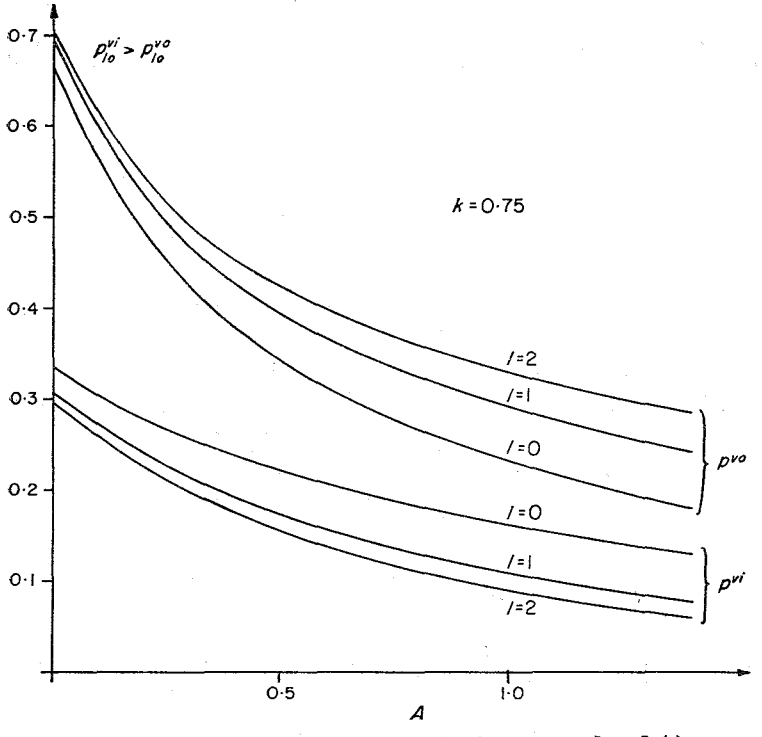

FIG. 4.—Transmission probabilities for sources $Q \sim f_i(r)$

The Figs. 3 and 4 show transmission probabilities for a cylindrical layer with $k = R_i/R_o = 0{\cdot}75$ as a function of $A = \Sigma(R_o - R_i)$. The dependence on the angular current resp. spatial source distribution is obviously quite remarkable.

3. TRANSMISSION PROBABILITIES FOR SPACE DEPENDENT ANISOTROPIC SCATTERING SOURCES IN PLANE GEOMETRY

For anisotropic scattering the cross section is approximated by a series of Legendre polynomials

$$\sum_s(\Omega', \Omega) = \frac{1}{4\pi} \sum_{m=0}^{M} s_m P_m (\cos(\Omega', \Omega)). \tag{6}$$

As a first step the angular distribution of the scattering source after the s'-th collision will be evaluated. As the anisotropic scattering is treated only for neutrons remaining in the same energy group, the formulas can be restricted to the monoenergetic case.

$$Q_s(r, \Omega) = \int \mathrm{d}\Omega' \sum_s (\Omega', \Omega)\Psi_{s-1}(\mathbf{r}, \Omega') \tag{7}$$

where $\psi_{s-1}(\mathbf{r}, \Omega')$ is the flux density of $s-1$ times scattered neutrons. For $s = 1$, ψ_0 is the density of the unscattered neutrons, which is a function of the ingoing current $j_i(\alpha) = \cos^i \alpha$. In plane geometry

$$\psi_0(r, \alpha) = \cos^{i-1}\alpha \exp\left(-\frac{Ax}{\cos \alpha}\right) \tag{8}$$

with $A = \Sigma \,.\, \Delta R$ and $x = r/\Delta R$, ΔR being the thickness of the layer and r the coordinate normal to the boundary. Combining equations (6)–(8) one finds

$$Q_1(x, \Omega) = \sum_{m=0}^{M} \frac{s_m}{2} \int P_m(\cos(\Omega', \Omega)) \cos^{i-1}\alpha' \sin \alpha' \exp\left(-\frac{Ax}{\cos \alpha'}\right) \mathrm{d}\alpha'$$

$$= \sum_{m=0}^{M} Q_1{}^m(x, \Omega). \tag{9}$$

Using

$$\cos(\Omega', \Omega) = \cos \alpha' \cos \alpha + \sin \alpha' \sin \alpha \cos(\phi - \phi') \tag{10}$$

one finds

$$Q_1{}^m(x, \Omega) = \frac{s_m}{2} P_m(\cos \alpha) \,.\, B_m(Ax) \tag{11}$$

with $B_m(Ax)$ given in Appendix 2. Similar to the treatment of the isotropic sources in plane geometry, the space dependent part will be approximated by a polynomial in x, while the angular dependence is treated rigorously. Thus

$$Q_1{}^m(x, \Omega) = \frac{s_m}{2} P_m(\cos \alpha) \,.\, \sum_{l=0}^{L} a_{l1}{}^m x^l \tag{12}$$

is used for the determination of the transmission probabilities. The flux density in x' due to the neutron source $Q_1(x, \Omega)$ is

$$\psi_1(x', \Omega) = \int \frac{\mathrm{d}x}{\cos \alpha} Q_1(x', \Omega) \exp\left(-\frac{A(x' - x)}{\cos \alpha}\right). \tag{13}$$

From (12) and (7) the source of twice scattered neutrons can be found. It turns out

to be separable in space and angle similar to $Q_1(x, \Omega)$:

$$Q_2(x, \Omega = \sum_{m=0}^{M} Q_2^m(x, \Omega)$$

with

$$Q_2^m(x, \Omega) = \frac{s_m}{2A} P_m(\cos\alpha) \sum_{l=0}^{L} \sum_{m'=0}^{M} \frac{s_{m'}}{2} a_{l1}^{m'} 0_l^{mm'}(x). \tag{14}$$

Formulas for $Q_l^{mm'}$ can be found in Appendix 2. As equation (14) shows the source $Q_2^m(x, \Omega)$ to be separable in space and angle, an approximation according to (12) is possible for this source and all subsequent scattering sources $Q_s^m(x, \Omega)$ as well. The coefficients a_{ls}^m are found with the help of $Q_s^m(0,\Omega)$, $Q_s^m(1, \Omega)$ and $\int_0^l dx\, Q_s^m(x,\Omega)$ as resulting from (11) for $s = 1$ and (14) for $s > 1$.

The remaining task is to calculate the transmission probabilities and their higher moments for the sources defined by (9) and (12). They are given by

$$P_{Q_s,j}^{v\to i} = \sum_{m=0}^{M} \frac{s_m}{s_0} \frac{\int d\Omega\, P_m(\cos\alpha) \int_0^1 dx \exp\left(\frac{-Ax}{\cos_\alpha}\right) \cos^j \alpha \sum_{l=0}^{L} a_{ls}^m x^l}{4\pi \int_0^1 dx \sum_{l=0}^{L} a_{ls}^0 x^l}$$

$$= P_{oj}^{v\to i} + \sum_{m=1}^{M} \frac{s_m}{s_0} P_{mj}^{v\to i}. \tag{15}$$

Similar relations hold for $P_{Q_s,j}^{v\to o}$. The definition of $P_{mj}^{v\to i}$ arising from (15) must not be confused with that for $P_{lj}^{v\to i}$ given in section 2; there, l refers to the spatial source component, while here m refers to the angular component, and the spatial distribution is treated as a whole. For $m > 0$, the resulting $P_{mj}^{v\to i}$ should not be interpreted as probabilities, but rather as corrections to $P_{oj}^{v\to i}$. Formulas for the probabilities are listed in Appendix 2.

4. TRANSMISSION AND REFLECTION MATRICES

The remaining task is to determine the transmission and reflection matrices S (equation (1)) from the transmission probabilities P. S depends on the definition of the current j, which will be taken to be the vector of the amplitudes of all group currents. Each component of j gives rise to one column of S.

In a first step the transmission and reflection probabilities and their moments are determined. It is assumed that after the s'th collision the spatial scattering source distribution has reached an asymptotic value which may be either space dependent or isotropic; the asymptotic angular source distribution is assumed to be isotropic. In this case, the contribution of all subsequent collisions can be summarized.

The transmission resp. reflection probabilities will be denoted by $P_{ij}^{2+}(m, n)$, $P_{ij}^{+-}(m, n)$ etc., where i and m are the component and the group number of the ingoing current, j is the moment, n the group number of the outgoing current, and the $+$ and $-$ signs refer to the direction of in- and outgoing current similar to the definition of S in (1). Further, $R_s^{i\pm}(m, n)$ is the probability for ingoing neutrons belonging to component i of group m to be in group n after the s'th collision with $+$ or $-$ referring to the direction of the ingoing current. R_s is a function of the transmission

probabilities for the 0 to $s-1$ times scattered neutrons. With these definitions

$$P_{ij}^{2+}(m, n) = P_{ij}^{i\to o}(n)\delta_{mn} + \sum_{s=1}^{\infty} R_s^{i+}(m, n)P_{Q_s^{i+}(m,n)}^{v\to 0}. \tag{16}$$

For the introduction of the asymptotic source all $P_{ij}^{2+}(m, n)$ with equal n have to be collected into a vector $\mathbf{P}_{ij}^{2+}(m)$ of order G. It can be written as

$$\mathbf{P}_{ij}^{2+}(m) = \sum_{s=0}^{\infty} \mathbf{V}_{s,ij}^{2+}(m) \tag{17}$$

where each $\mathbf{V}$ refers to one term in (16). In keeping these symbols $\mathbf{V}$ for the first $S-1$ collisions and summarizing the rest, (17) becomes:

$$\mathbf{P}_{ij}^{2+}(m) = \sum_{s=0}^{S-1} \mathbf{V}_{s,ij}^{2+}(m) + P_\infty{}^{j}(E - N_\infty)^{-1}\mathbf{R}_S{}^{i+}(m). \tag{18}$$

Here, $\mathbf{R}_S{}^{i+}(m)$ is the vector of all $R_S{}^{i+}(m, n)$, E is the unitary matrix, and $P_\infty{}^{j}$ and N are matrices of order G:

$$P_\infty{}^{j} = \operatorname{diag}\,(P_{Q_\infty(n),j}^{v\to o})$$

$$N_\infty = \left(\frac{\sum_s^{m\to n}}{\sum^m}\,(1 - P_{Q_\infty(m),0}^{v\to o} - P_{Q_\infty(m),0}^{v\to i})\right).$$

$Q_\infty(m)$ is the asymptotic source distribution in group m, which may depend on component, group, and direction of the ingoing current. Similar formulas hold for $P_{ij}{}^{+-}(m, n)$ etc.

The second step consists of a normalization of P such that the results of a multiplication with the components of the ingoing current are the components of the outgoing current. The normalization must take into account

(a) that the inner and outer surface of cylindrical and spherical layers are not equal
(b) that the functions $\cos^i \alpha$ are not normalized
(c) that the moments of the probabilities have to be transformed so as to give the contributions to the different components.

The results of the normalization are the matrices S of equation (1).

Extraneous sources, which will be denoted by E, are treated similarly to scattering sources. The results are the components $P_{E,j}^{+}(n)$, $P_{E,j}^{-}(n)$ of two vectors of the escape probabilities for the source, and their moments. The normalization consists of

(a) multiplication with the total source (integrated over the layer);
(b) multiplication with a factor effecting the transformation from a volume source to a current;
(c) the same operation as in (c) above.

The results are the source vectors R^+ and R^- of equation (1). Details on the normalizations may be found in the work of MAYER (1968).

5. SOLUTION OF MULTI-LAYER PROBLEMS AND COMBINATION WITH DIFFUSION THEORY

After the determination of S and R, equations (1) can be solved together with the proper boundary conditions. These depend on the nature of the problem and will be given below for some common cases. Subscripts refer to the number of the layer.

(a) Spherical or cylindrical cell. Here, the inner boundary is non-existent and

equation (1) for the innermost layer reduces to

$$\mathbf{j}_1^+ = S_1^{-+}\mathbf{j}_1^- + \mathbf{R}_1^+. \tag{19}$$

At the outer boundary, one may impose a boundary condition of the form

$$\mathbf{j}_N^- = A\mathbf{j}_N^+. \tag{20}$$

If A is a unitary matrix, this is a reflecting boundary condition, but A can be defined so as to give the "white" boundary condition or any other type of reflection.

(b) Plane cell. Here one has to distinguish between symmetric and non-symmetric cells. An example of the first case is the sequence of layers *abcbabcba* . . .. It is sufficient to treat the layers $a/2$, b, $c/2$ and the boundary conditions are

$$\begin{aligned} \mathbf{j}_0^+ - \mathbf{j}_0^- &= 0 \\ \mathbf{j}_N^+ - j_N^- &= 0. \end{aligned} \tag{21}$$

An example for the non-symmetric case is the sequence *abcabc* . . . , for which one has to treat the layers a, b, c with the boundary conditions

$$\begin{aligned} \mathbf{j}_N^+ &= \mathbf{j}_0^+ \\ \mathbf{j}_N^- &= \mathbf{j}_0^- \end{aligned} \tag{22}$$

This gives rise to a special system of equations which has to be solved with a special technique.

(c) Whole assemblies are formally treated as cells. In this case, the ingoing current at the outer boundary is often required to be zero, which means putting $A = 0$ in (20).

(d) Flux distributions in layers with a source at the left boundary. The boundary condition at the left boundary is normally

$$\mathbf{j}_0^+ - \mathbf{j}_0^- = \mathbf{g}_0 \tag{23}$$

but might be

$$\mathbf{j}_0^+ = \mathbf{g}_0. \tag{24}$$

The second case refers to vacuum to the left of the layer and a source at the boundary, while in the first case flux and flux gradient at the left boundary are known. For the right boundary (20) applies.

(e) Combination with diffusion theory. In this case, the results of foregoing diffusion calculations for the whole geometry are used to provide the vector $\mathbf{g}_0$ for (23) and/or $\mathbf{g}_N$ for a similar condition for the outer boundary. If one boundary of the section to be recalculated with transport theory coincides with the inner or outer boundary of the whole system, the proper boundary condition, e.g. (19) or (20), is applied. The "coupling" points, at which (23) is used, have to be chosen in a region where diffusion theory is valid; there

$$\psi(\Omega) = \frac{\phi}{4\pi} - \frac{3}{4\pi} D \operatorname{grad} \phi \cos \alpha \tag{25}$$

is used for the determination of $\mathbf{g}$. A deviation of diffusion and transport calculation results at the coupling point indicates that (25) is not valid there.

The system of matrix equations arising from (1) and the boundary conditions except (28) is tridiagonal and can be solved without iteration. An estimate of computing times for different numerical techniques has indicated that this method is indeed the least time consuming one. Nevertheless the normal line inversion had to be slightly modified for numerical purposes. The following recursive relations are used in this modification:

$$\mathbf{j}_{i-1}^{-} = \mathbf{F}_i^{-} + G_i^{-}\mathbf{j}_i^{-} \qquad \text{(normally } \mathbf{j}_{i-1}^{-} = \mathbf{F}_i^{-} + G_i^{-}\mathbf{j}_i^{+} \text{ with, of course,}$$

$$\mathbf{j}_i^{+} = \mathbf{F}_i^{+} + G_i^{+}\mathbf{j}_i^{-} \qquad \text{other relations for } \mathbf{F}_i \text{ and } G_i).$$

From equation (1)

$$G_i^{-} = (E - S_i^{+-}G_{i-1}^{+})^{-1}S_i^{2-}$$
$$\mathbf{F}_i^{-} = (E - S_i^{+-}G_{i-1}^{+})^{-1}(\mathbf{R}_i^{-} + S_i^{+-}\mathbf{F}_{i-1}^{+})$$
$$G_i^{+} = S_i^{-+} + S_i^{2+}G_{i-1}^{+}G_i^{-}$$
$$\mathbf{F}_i^{+} = \mathbf{R}_i^{+} + S_i^{2+}(\mathbf{F}_{i-1}^{+} + G_{i-1}^{+}\mathbf{F}_i^{-})$$

where E is the unitary matrix. G_0^{+} and $\mathbf{F}_0^{+}$ are derived from the left boundary condition, $\mathbf{j}_N^{-}$ from the right one.

In the case of the non-symmetric plane cell the system of the matrix equations is nearly tridiagonal with a few non-zero elements in the upper right corner of the matrix. The line inversion technique can be modified so as to handle this problem too. One applies the recursion relations

$$\mathbf{j}_i^{+} = G_i^{+}\mathbf{j}_N^{-} + H_i^{+}\mathbf{j}_N^{+} + \mathbf{F}_i^{+}$$
$$\mathbf{j}_i^{-} = G_i^{-}\mathbf{j}_N^{-} + H_i^{-}\mathbf{j}_N^{+} + \mathbf{F}_i^{-}.$$

For $1 \leq i < N$

$$G_i^{-} = -(S_i^{2-})^{-1}(S_i^{+-}G_{i-1}^{+} - G_{i-1}^{-})$$
$$H_i^{-} = -(S_i^{2-})^{-1}(S_i^{+-}H_{i-1}^{+} - H_{i-1}^{-})$$
$$\mathbf{F}_i^{-} = -(S_i^{2-})^{-1}(\mathbf{R}_i^{-} + S_i^{2+}\mathbf{F}_{i-1}^{+} - \mathbf{F}_{i-1}^{-})$$
$$G_i^{+} = S_i^{2+}G_{i-1}^{+} + S_i^{-+}G_i^{-}$$
$$H_i^{+} = S_i^{2+}H_{i-1}^{+} + S_i^{-+}H_i^{-}$$
$$\mathbf{F}_i^{+} = \mathbf{R}_i^{+} + S_i^{2+}\mathbf{F}_{i-1}^{+} + S_i^{-+}\mathbf{F}_i^{-}$$

with, for $i = 1$

$$G_0^{+} = H_0^{+} = E \qquad G_0^{-} = H_0^{-} = \mathbf{F}_0^{-} = \mathbf{F}_0^{+} = 0$$

$\mathbf{j}_N^{-}$ and $\mathbf{j}_N^{+}$ are the solutions of the system

$$A\mathbf{j}_N^{+} + B\mathbf{j}_N^{-} = \mathbf{U}; \quad C\mathbf{j}_N^{+} + D\mathbf{j}_N^{-} = \mathbf{F}$$

with

$$A = G_{N-1}^{-} - S_N^{+-}G_{N-1}^{+}; \quad B = H_{N-1}^{-} - S_{N-1}^{+-}H_{N-1}^{+} - S_N^{2-}$$
$$C = E - S_N^{2+}G_{N-1}^{+}; \quad D = -S_N^{2+}H_{N-1}^{+} - S_N^{-+}$$
$$\mathbf{U} = \mathbf{R}_N^{-} - \mathbf{F}_{N-1}^{-} + S_N^{+-}\mathbf{F}_{N-1}^{+}; \quad \mathbf{V} = \mathbf{R}_N^{+} + S_N^{2+}\mathbf{F}_{N-1}^{+}.$$

After the determination of the currents, the fluxes at the boundary are determined

from the currents via $\psi(\Omega) = j(\Omega).\cos\alpha$ and the mean fluxes in the layer by using a balance equation.

It should be mentioned that the collision probability code STOWA, which has been written for the application of the techniques developed herein, is coupled to the Karlsruhe nuclear code system NUSYS. This enables the user to run a problem fully automated, beginning with the determination of group cross sections and, if necessary, the foregoing diffusion calculation and then starting the collision probability code. Because of the small computer memory of the IBM 7074 the following restrictions have to be observed:

$$M \leq 3;\ I \leq 4;\ G \leq 12;\ I.G \leq 16;\ I.G.(N+1) \leq 1536.$$

6. RESULTS

1. Cell calculations. The first example is a relatively crude seven-group calculation of the flux distribution in a cylindrical thermal reactor cell; it serves to determine the effects of the generalizations. The geometry is that of the Wigner–Seitz-cell of the FR2, which originally consists of a cluster of seven fuel pins. For our purpose the six outer pins have been cylindricized so as to obtain cylindrical geometry. The successive layers may be derived from Figs. 5 or 6.

Figure 5 shows the effects of the detailed source and flux treatment on the flux distribution in the thermal group. While there is a large difference in the flux distributions for the constant source approximation and the space dependent source, the DP_N-approximation has no large effect in this case. The last effect gets bigger in the high energy groups as might be expected but does not alter the fast fission factor ε appreciably. ε and the disadvantage factor d are given for different approximations in Tables 1 and 2.

Further calculations with this example have been done in order to determine the allowable zone width and the necessary number of source approximations for the successive collisions. The zone width may be up to one mean free path for materials with scattering out-weighing absorptions and bigger for materials with absorption exceeding the scattering. The space dependence of the source should be determined for up to the third collision for these zone widths. The accuracy of calculations with zone widths of one mean free path is comparable to that of S_n- and P_n-calculations with meshes of 0·3 mean free paths; for collision probability calculations with the constant source approximations this value is even less.

As the code handles different boundary conditions, the results for a reflecting and a white boundary have been compared. In the thermal group the flux varies by about 4 per cent at the outer boundary, but the disadvantage factor is only changed to 1·66 for the white boundary as compared to 1·67 from Table 1 for the reflecting boundary. A one group calculation for the thermal group only has been done as well using an idealized source of downscattered neutrons: $Q = 1$ in the moderator and coolant and $Q = 0$ elsewhere. This is a widely used assumption for thermal cell calculations. A comparison of the resulting thermal flux with that from the 7-group-calculation shows no differences.

As an example for adjoint calculations which can be handled as well, Fig. 6 shows the adjoint fluxes in some groups for the foregoing cell problem.

Heterogeneity calculations for fast reactors have been performed too, but the

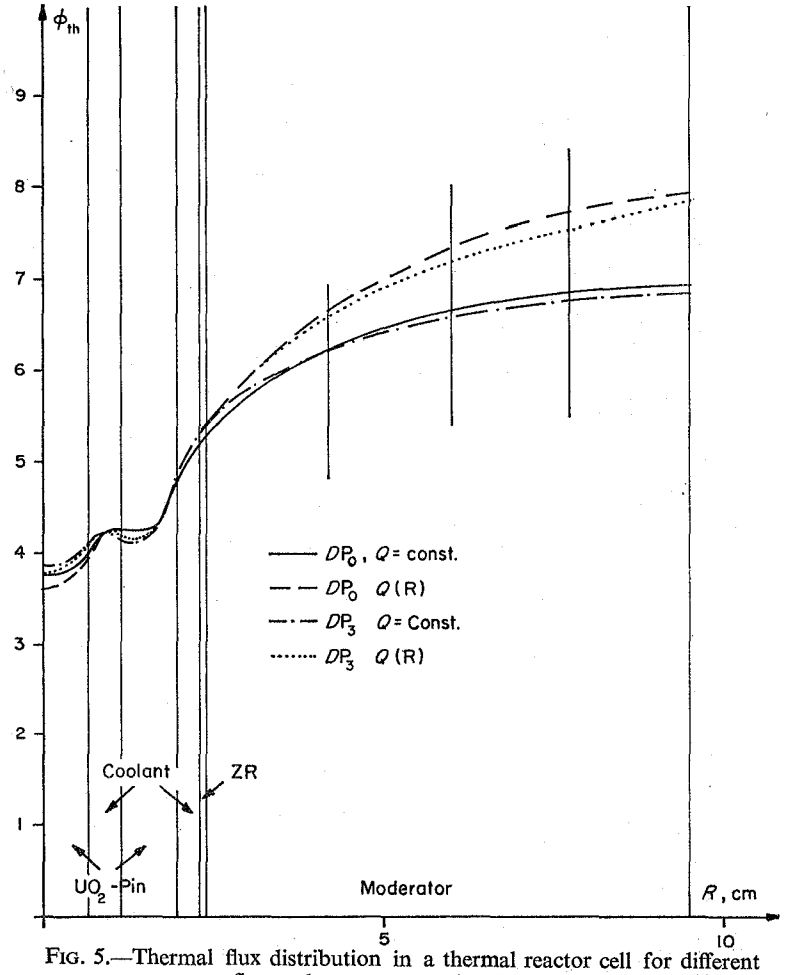

FIG. 5.—Thermal flux distribution in a thermal reactor cell for different flux and source approximations.

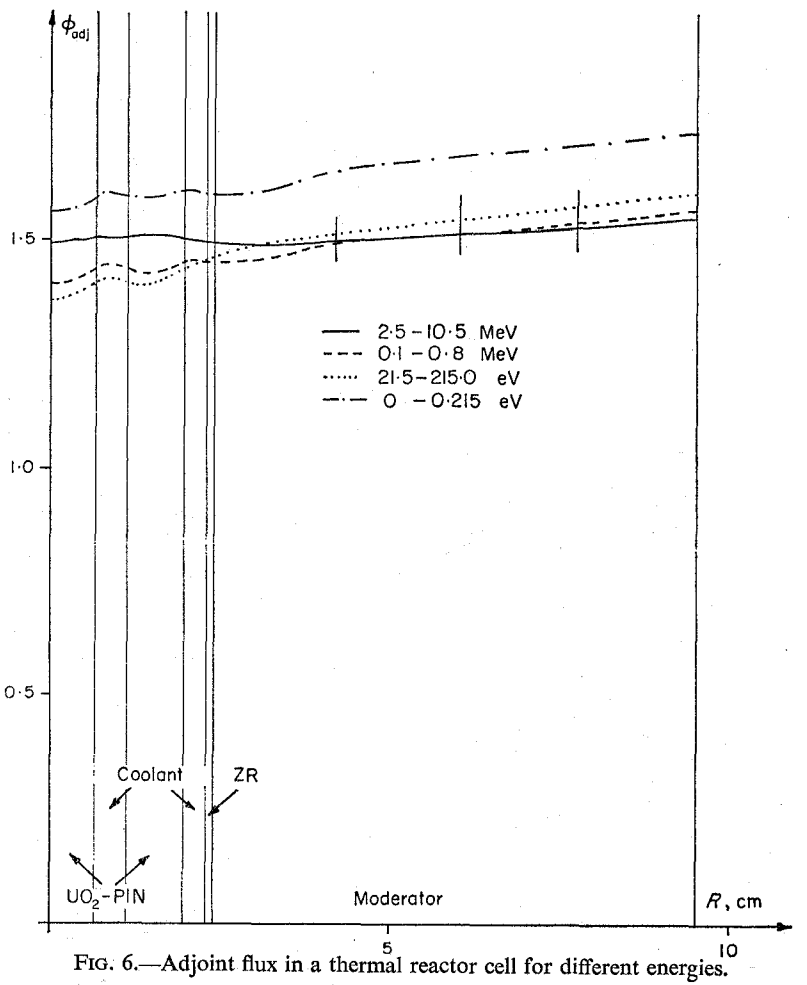

FIG. 6.—Adjoint flux in a thermal reactor cell for different energies.

TABLE 1.—DISADVANTAGE FACTOR FOR THE DIFFERENT APPROXIMATIONS

flux \ source	Q = const	$Q(r)$
DP_0	1·56	1·70
DP_3	1·52	1·67

TABLE 2.—FAST FISSION FACTOR FOR DIFFERENT FLUX APPROXIMATIONS

flux	ε
DP_0	1·0104
DP_1	1·0108
DP_2	1·0113
DP_3	1·0116

effects of self-shielding have to be included in the group constants before the calculation starts. If average self-shielding factors for the layers are used, this leads to rather good results for flux distributions and average reaction rates, but does not yield information on the distribution of the reaction rates in individual layers in the resonance groups.

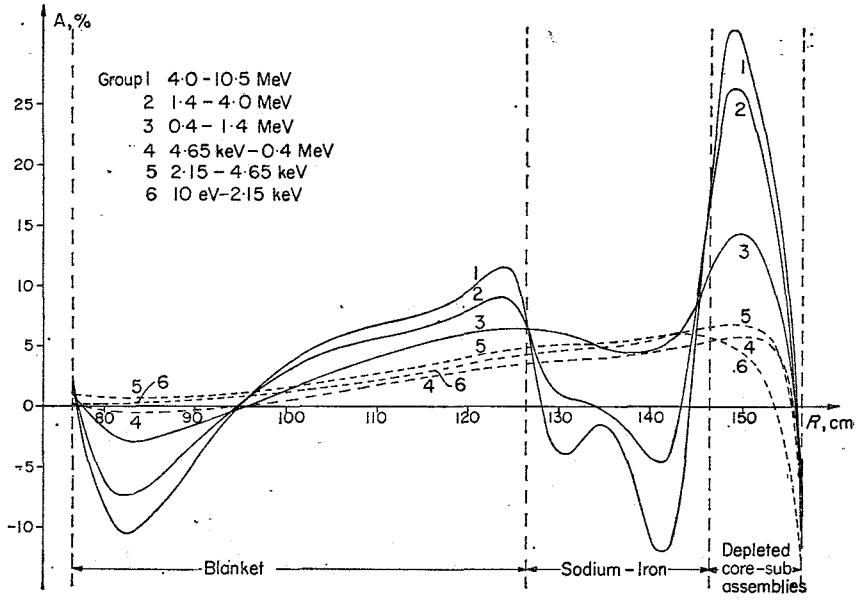

FIG. 7.—Relative flux difference A for diffusion and collision probability calculation.

2. Blanket calculations. As an example for the coupling between diffusion and transport calculations, Fig. 7 shows the relative differences of the flux distributions in the blanket of a sodium-cooled fast reactor according to diffusion theory and collision probabilities. The coupling point is 5·15 cm to the left of the blanket. The largest effects occur in the fast groups, and one can easily classify the different transport effects contributing to Fig. 7:

1. Diffusion theory underestimates the flux gradient at boundaries between materials with different fission cross sections. This results in an underestimate by diffusion theory of the fluxes on the side with the bigger fission cross section and an overestimate on the other side.
2. Diffusion theory cannot predict the flux distribution near the outer boundary.

3. Diffusion theory underestimates the high energy neutron flux far away from sources. This error is due to the high forward peaking of the fast neutrons; it increases with increasing distance from the core and, at greater distances, effects the low energy flux as well by the downscattering.

The calculations have shown that the code is easily applicable to blanket problems, but that transport effects are too small to have an appreciable effect on the blanket

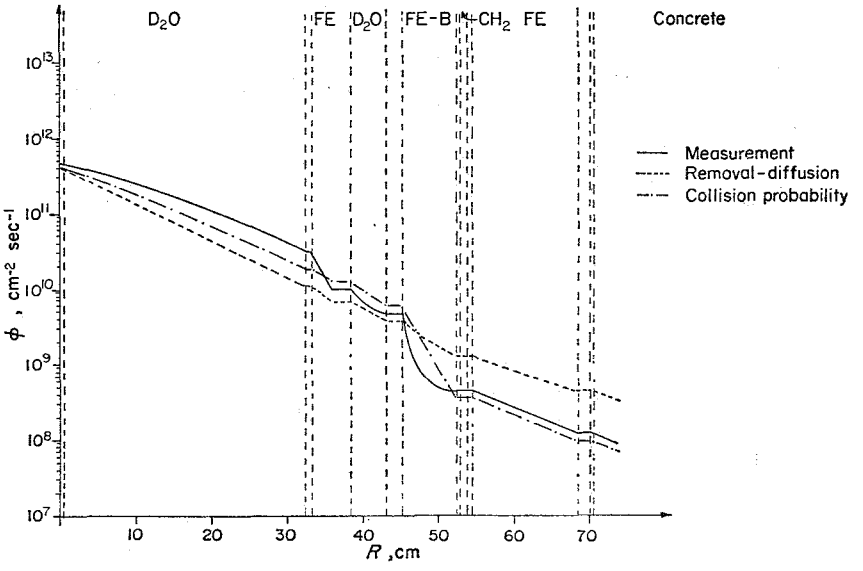

FIG. 8.—Intermediate flux distribution in a shielding model; 0·6 eV $\leq E \leq$ 1 MeV.

economics. Nevertheless, as shown by Fig. 7, transport effects evidently influence fluxes and flux gradients in the outer layers. Thus, such calculations are very important as input for shielding calculations.

A study of the flux distributions as a function of the angular flux approximation shows that for a blanket at least a DP_1 approximation has to be applied, while DP_3 is not necessary.

3. Shielding calculations. The accuracy of the code, especially for thick layers, has been tested against an experiment and a Monte Carlo calculation. The experiment is a measurement on the model of a reactor shield, which has been performed by SCHULTZ *et al.* (1967) at the experimental reactor in Geesthacht. The horizontal and vertical flux distributions have been determined in plane layers of different materials (e.g. Fig. 8) for different neutron energies. As the code can handle only one dimensional geometries, the transverse flux distributions have been used to determine transverse bucklings which account for the leakage. The results of the measurements, a removal-diffusion calculation and the collision probability code are given in Figs. 8 and 9 for the epithermal and the highest energies. There is an excellent agreement between measurement and calculations. It should be stressed that no removal-diffusion concept has been employed in the collision probability code; the cross sections were condensed from the 26-group set by ABAGJAN *et al.* (1964) with, for

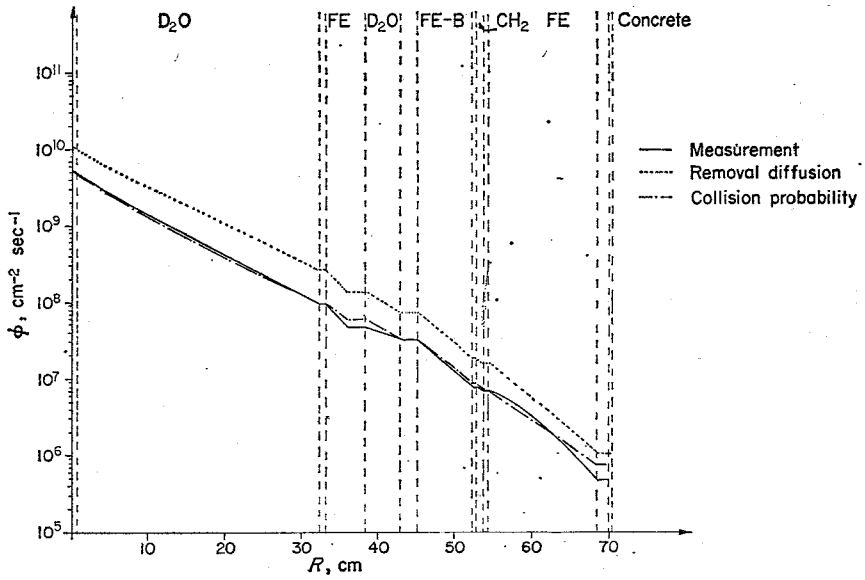

FIG. 9.—Fast flux distribution in a shielding model; $E > 6$ MeV.

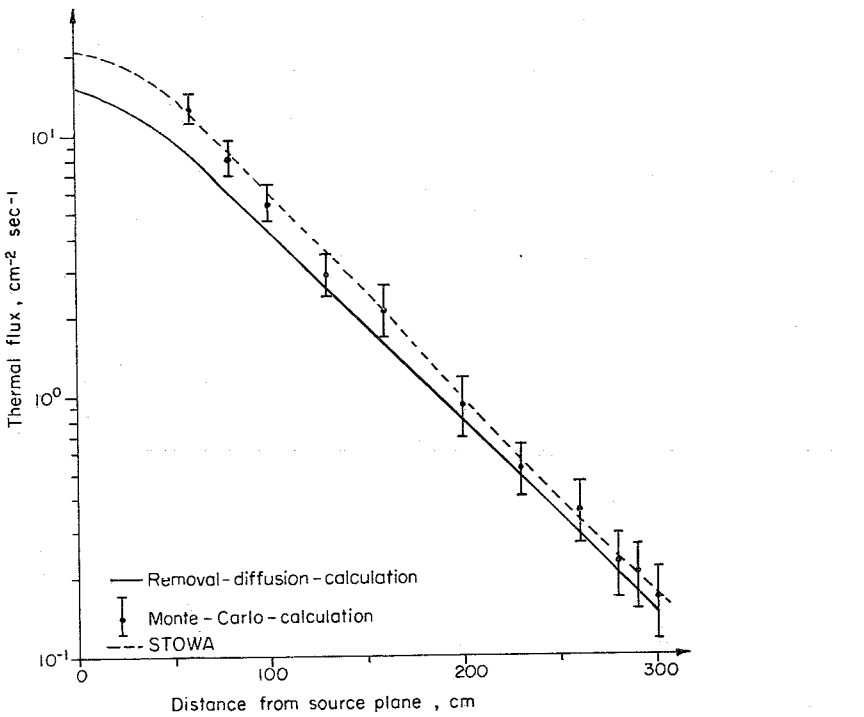

FIG. 10.—Thermal flux in graphite due to a 5 MeV source.

the transport cross section in group g

$$\Sigma_{tr}^{g} = \Sigma_{tot}^{g} - \mu^{gg}\Sigma_{i}^{gg} \qquad \text{(see section 7).}$$

As for the removal-diffusion calculations reported by SCHULTZ *et al.* (1967), they were done for the whole geometry including the core and there gave too high fluxes in the high energy region; this gives rise to the generally too high results in Fig. 9.

The second example is the determination of the flux distribution due to an infinite plane source of high energy neutrons in the middle of a carbon layer of 7 m thickness. The Monte Carlo calculations were done by BENDALL and MCCRACKEN (1967). The results for the thermal flux (Fig. 10) show an excellent agreement of STOWA and Monte Carlo results. Flux distributions for higher energies were not available.

7. EVALUATION OF DIFFERENT SCATTERING MODELS FOR LIGHT NUCLEI

As the code is able to handle a P_N-approximation for the angular dependence of the scattering (in one group), it has been used to evaluate the different approximations to angular scattering. The application of the transport approximation in transport theory offers some problems for the lightest nuclei because it leads to negative scattering cross sections for scattering in one group, if the group is sufficiently small. For hydrogen, "sufficiently small" groups really include quite broad groups; for example for a $1/E$-flux the scattering cross section becomes negative for $\Delta u \leq 2{,}8$. For an illustration see Fig. 11 which depicts the true angular dependence of neutrons scattered on hydrogen in an energy group with $\Delta u = 1{\cdot}39$ and the different approximations. Clearly, the transport approximation is very far off the mark.

For a quantitative comparison the neutron flux in a layer of 70 cm thickness containing only hydrogen with a density of $1{\cdot}6 \cdot 10^{22}$ cm^{-3} and with a plane infinite source of high energy neutrons on one side has been calculated using the different approximations. Six energy groups were used, taking very coarse groups in the low and intermediate energy region and three high energy groups. Taking the P_3 results as a standard, the deviations of the fluxes at the outer boundary of the layer are

0–0·1 %	for the P_1 and P_2 approximation,
5 %	for the isotropic approximation,
40 %	for the transport approximation,
1–2 %	for the modified transport approximation.

These calculations show surprisingly good results for the modified transport approximation, which leaves the mean cosine for scattering in one group, $\mu^{i\to i}$, unaltered:

$$\Sigma_{tr}^{i\to i} = \Sigma_{tot}^{i} - \Sigma_{s}^{i\to i}\,\mu^{i\to i};\quad \Sigma_{s,tr}^{i\to i} = \Sigma_{s}^{i\to i}\,(1 - \mu^{i\to i}).$$

Thus in multigroup transport calculations with light nuclei, this approximation should be preferred to the normal transport approximation, if one does not wish to use a P_N-approximation. This is of special significance for transport calculations in weakly or non-multiplying media, in which the normal transport approximation gives very poor results. For example, the shielding calculations have been done with the modified transport approximation; with the normal transport approximation the fast flux distribution (Fig. 9) is much flatter.

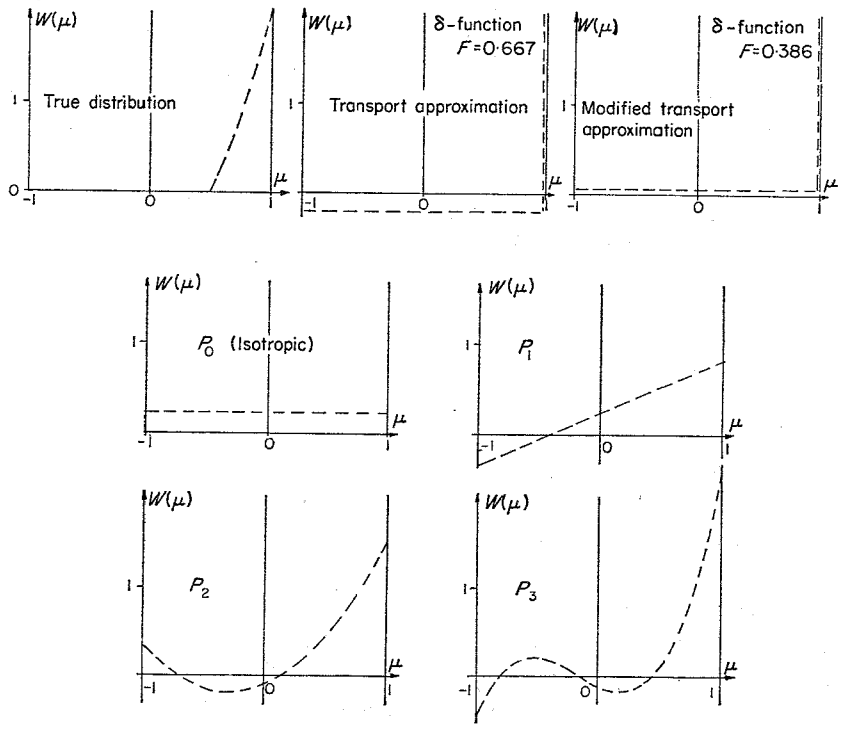

FIG. 11.—True angular distribution of neutrons scattered on hydrogen in a group with $\Delta u = 1{\cdot}39$ and different approximations.

It should be stressed, that the results of this investigation are valid only for relatively broad energy groups for which the angular downscattering is approximately isotropic, as the angular dependence of downscattering has not been treated.

8. CONCLUSIONS

The extension of the multiple collisions method to space dependent scattering sources and a DP_N-approximation for fluxes in the multigroup approximation has proven to yield extremely accurate results for a much coarser mesh than that necessary for other transport methods with equal accuracy. For plane geometry, the formalism has been extended to include anisotropic scattering. These extensions seem to be the limit of what can be achieved with multiple collision probabilities as the numerical work is formidable and becomes even more so for any further extension.

The effect of the extensions on the different types of calculations are as follows:

1. Cell calculations: The isotropic flux approximation proves to be satisfactory while the space dependent source approximation shows a considerable effect on flux distributions. Naturally, with a constant source and finer mesh this effect may be taken into account, but there is a limit to the fineness of the mesh imposed by growing numerical errors.
2. Blanket calculations: Transport effects in the layers near the core can be handled very easily by combining the method with a diffusion code. The use of space dependent sources in this case is vital in order to avoid big numbers of

mesh points. The results are valuable as boundary conditions for shielding calculations while there are no appreciable effects on blanket economics.

3. Shielding calculations: Comparison with measurements and Monte Carlo calculations show excellent agreement with collision probability calculations for thicker layers (about 50 mean free paths) without making use of the removal diffusion concept.

Acknowledgments—The author would like to express her gratitude to Professor K. Wirtz for support of the work and to Dr. H. Küsters for many useful discussions.

REFERENCES

AMOUYAL A., BENOIST P. and HOROWITZ J. (1957) *J. nucl. Energy* **6**, 79.
GAST P. F. (1962) *Trans. Am. nucl. Soc.* **5**, 351.
SAHNI D. C. (1966) *Proceedings of the Nuclear Physics and Solid State Physics Symposium*, Bombay.
SYROS C. (1966) *Nukleonik* **8**, 467.
SYROS C. (1967) *Nucl. Sci. Engng* **28**, 203.
KIER P. H. (1966) *Nucl. Sci. Engng* **26**, 230.
KIER P. H (1967) AED-Conf 1967-069-020; *International Conference on the Utilization of Research Reactors and Reactor Mathematics and Computation*, Mexico City.
MURLEY T. E. and KAPLAN I. (1967) *Nukleonik* **10**, 177.
MÜLLER A. and LINNARTZ E. (1963) *Nukleonik* **5**, 23.
MAYER L. (1968) Kernforschungszentrum Karlsruhe, Externer Bericht 4/68-21 (Thesis).
BICKLEY W. G. and NAYLER J. (1935) *Phil. Mag.* **20**, Ser. 7, 343.
HÖRTNER H. and PUTZ F. (1968): *SGAE RT*-17/1968.
SCHULTZ H. *et al.* (1967) *Nukleonik* **9**, 1.
BENDALL D. E. and MCCRACKEN A. K. (1967) *International Conference on the Physics Problems of Reactor Shielding*, Harwell (unpublished).
ABAGJAN L. P., BAZAZJANC N. O., BONDARENKO I. I. and NIKOLAEV M. N. (1964) Moskau (1964) and KFK-tr-144.

APPENDIX 1

Transmission probabilities for anisotropic fluxes and space dependent scattering sources

The transmission probabilities for surface and volume source neutrons will be listed below for the different geometries using the following abbreviations:

R_i inner, R_0 outer radius of G;

$A = \sum(R_0 - R_i)$; $A' = \dfrac{A}{1-k}$ $(k \neq 1)$;

$k = R_i/R_0$; $k = 1$: plane geometry.

At first, the transmission probabilities $P^{o\to i}$, $P^{i\to o}$ and $P^{o\to o}$ for surface sources, i.e. ingoing currents from the in- and outside of G will be given. Subscripts i $(i = 1 \ldots \mathrm{I})$ and j $(j = 0 \ldots \mathrm{I} - 1)$ denote the flux component and the moment of the probability. Plane geometry:

$$P_{ij}^{o\to o} = 0$$

$$P_{ij}^{o\to i} = P_{ij}^{i\to o} = (i+1)Ei_{i+j+2}(A)$$

with

$$Ei_m(x) = \int_1^\infty e^{-xt} \cdot \frac{\mathrm{d}t}{t^m}$$

Cylindrical geometry:

$$P_{ij}^{o\to o} = \frac{2(i+1)}{\pi}\int_k^1 \mathrm{d}y\sqrt{1-y^2}^{i+j-1}\,.\,Ki_{i+j+2}(2A'\sqrt{1-y^2})$$

$$P_{ij}^{i\to o} = \frac{2(i+1)}{\pi}\int_k^1 \mathrm{d}y\sqrt{1-y^2}^{j}\sqrt{1-\frac{y^2}{k^2}}^{i-1}\,.\,Ki_{i+j+2}(A'(\sqrt{1-y^2}-\sqrt{k^2-y^2})$$

$$P_{ij}^{o\to i} = \frac{i+1}{j+2}kP_{j+1,i-1}^{i\to o}$$

with Ki_m denoting the Bickley-function (BICKLEY *et al.*, 1935)

$$Ki_m(x) = \int_1^\infty e^{-xt}\frac{\mathrm{d}t}{t^m\sqrt{1-t^2}}.$$

Spherical geometry:

$$P_{ij}^{o\to o} = (i+1)M_{i+j}$$

$$P_{ij}^{i\to o} = \frac{i+1}{k^{i+1}}\int_0^k \mathrm{d}y\,.\,y\sqrt{k^2-y^2}^{i-1}\sqrt{1-y^2}^{j}\exp\left(-A'(\sqrt{1-y^2}-\sqrt{k^2-y^2})\right)$$

$$P_{ij}^{o\to i} = \frac{i+1}{j+2}k^2P_{j+1,i-1}^{i\to o}$$

with

$$M_0 = \frac{1}{2A'}(1-\exp(-2A'\sqrt{1-k^2}))$$

$$M_m = \frac{1}{2A'}(mM_{m-1}-\sqrt{1-k^2}^m\exp(-2A'(\sqrt{1-k^2})).$$

The integrals for cylindrical and spherical geometry have to be evaluated numerically.

For the volume sources, the transmission probabilities $P^{v\to o}$ and $P^{v\to i}$ will be given with l denoting the space dependent term in the source approximation and j the moment of the probability.

Plane geometry:

$$P_{lj}^{v\to i} = (l+1)\int_0^1 \mathrm{d}x x^l Ei_{j+2}(Ax)$$

$$P_{0j}^{v\to o} = P_{0j}^{v\to i}$$

$$P_{1j}^{v\to o} = 2P_{0j}^{v\to i} - P_{1j}^{v\to i}$$

$$P_{2j}^{v\to o} = P_{2j}^{v\to i} + 3(P_{0j}^{v\to i} - P_{1j}^{v\to i}).$$

The integral can be evaluated analytically.

Cylindrical geometry:

$$P_{lj}^{v\to o} = P_{lj}^{v\to o1} + P_{lj}^{v\to o2}$$

$$P_{lj}{}^u = \frac{l+1}{\pi(1-k^2)^{l+1}}\int_{y_1}^{y_2}\mathrm{d}y\int_0^\pi \mathrm{d}\alpha\sin^{j+1}\alpha\int_{x_1}^{\sqrt{1-y^2}}\mathrm{d}x f(y)\,.\,(x^2+y^2-k^2)^l$$

$$\exp\left(-\frac{A'}{\sin\alpha}\,.\,z(x,y)\right)$$

where y_1, y_2, x_1, f and z assume the following values for the different u's:

u	y_1	y_2	x_1	$f(y)$	$z(x, y)$
$v \to o1$	0	k	$\sqrt{k^2 - y^2}$	$\sqrt{1 - y^2}^j$	$\sqrt{1 - y^2} - x$
$v \to o2$	k	1	$\sqrt{1 - y^2}$	$\sqrt{1 - y^2}^j$	$\sqrt{1 - y^2} - x$
$v \to i$	0	k	$\sqrt{k^2 - y^2}$	$\sqrt{1 - y^2/k^2}^j$	$x - \sqrt{k^2 - y^2}$

The integrals over x and α can be evaluated analytically and by introducing the Bickley functions. The resulting single integrals, which must be solved numerically, are quite lengthy and may be found in detail in the work by MAYER (1968).
Spherical geometry:

$$P_{ij}{}^u = N_l \int_{y_1}^{y_2} \mathrm{d}y y \int_{x_1}^{\sqrt{1-y^2}} \mathrm{d}x (x^2 + y^2 - k^2) \,.\, f(y) \exp\,(-A' \,.\, z(x, y))$$

with the same definitions as for cylindrical geometry and with

$$N_l = (2(1 - k)^{l+1} F_l)^{-1}$$

$$F_0 = \tfrac{1}{3}\,(1 + k + k^2); \qquad F_1 = \frac{1}{3 \cdot 5}\,(3 + 6k + 4k^2 + 2k^3)$$

$$F_2 = \frac{1}{3 \,.\, 5 \cdot 7}\,(15 + 45k + 48k^2 + 24k^3 + 8k^4).$$

As for cylindrical geometry, the integration is performed analytically over x and numerically over y, and the single integral can be found in the work of MAYER (1968).

The informations on the space distribution of the scattering sources provided by the transmission probabilities will be given with Q referring to the total source, $Q(R_i)$ and $Q(R_0)$ to the source at the inner and outer boundary, and s denoting the number of collisions and i the component of the ingoing current:

Current from interior	Current from exterior
$Q_1(R_i) \sim 1$	$Q_1(R_i) \sim \frac{1}{k^p} P^{o \to i}_{i-1,0}$
$Q_1(R_0) \sim k^p \,.\, P^{i \to o}_{i-1,0}$	$Q_1(R_0) \sim 1 + P^{o \to o}_{i-1,0}$
$Q_1 \sim \frac{i}{i+1} \frac{1}{A} (1 - P^{i \to o}_{i,0})$	$Q_1 \sim \frac{i}{i+1} \frac{1}{A} (1 - P^{o \to i}_{i,0} - P^{o \to o}_{i,0})$

$$\left.\begin{aligned} Q_s(R_i) &\sim \frac{1}{k^p} P^{v \to i}_{Q_{s-1},-1} \\ Q_s(R_0) &\sim P^{v \to o}_{Q_{s-1},-1} \\ Q_s &\sim \frac{2}{A} (1 - P^{v \to i}_{Q_{s-1},0} - P^{v \to i}_{Q_{s-1},0}) \end{aligned}\right\} \quad s > 1$$

with $p = 0$ for plane, $p = 1$ for cylindrical, and $p = 2$ for spherical geometry.

APPENDIX 2

Spatial source distributions and transmission probabilities for anisotropic scattering in plane geometry

According to (11) the exact source distribution after one scattering is given by

$$Q_1{}^m(x, \Omega) = \frac{s_m}{2} P_m(\cos\alpha) \,.\, B_m(Ax).$$

An evaluation of (9) results in

$$\begin{aligned}
B_0(Ax) &= Ei_{i+1}(Ax)\\
B_1(Ax) &= Ei_{i+2}(Ax)\\
B_2(Ax) &= \tfrac{3}{2}Ei_{i+3}(Ax) - \tfrac{1}{2}Ei_{i+1}(Ax)\\
B_3(Ax) &= \tfrac{5}{2}Ei_{i+4}(Ax) - \tfrac{3}{2}Ei_{i+2}(Ax)
\end{aligned}$$

where i is the component of the ingoing current. For all subsequent collisions the source is given by (14) with the following functions $0_l^{mm'}(x)$:

$$\begin{aligned}
\mathrm{O}_l{}^{00}(x) &= F_l{}^+(2, x)\\
\mathrm{O}_l{}^{01}(x) &= \mathrm{O}_l{}^{10}(x) = F_l{}^-(3, x)\\
\mathrm{O}_l{}^{02}(x) &= \mathrm{O}_l{}^{20}(x) = \tfrac{3}{2}F_l{}^+(4, x) - \tfrac{1}{2}F_l{}^+(2, x)\\
\mathrm{O}_l{}^{03}(x) &= \mathrm{O}_l{}^{30}(x) = \tfrac{5}{2}F_l{}^-(5, x) - \tfrac{3}{2}F_l{}^-(3, x)\\
\mathrm{O}_l{}^{11}(x) &= F_l{}^+(4, x)\\
\mathrm{O}_l{}^{12}(x) &= \mathrm{O}_l{}^{21}(x) = \tfrac{3}{2}F_l{}^-(5, x) - \tfrac{1}{2}F_l{}^-(3, x)\\
\mathrm{O}_l{}^{13}(x) &= \mathrm{O}_l{}^{31}(x) = \tfrac{5}{2}F_l{}^+(6, x) - \tfrac{3}{2}F_l{}^+(4, x)\\
\mathrm{O}_l{}^{22}(x) &= \tfrac{9}{4}F_l{}^+(6, x) - \tfrac{3}{2}F_l{}^+(4, x) + \tfrac{1}{4}F_l{}^+(2, x)\\
\mathrm{O}_l{}^{23}(x) &= \tfrac{15}{4}F_l{}^-(7, x) - \tfrac{7}{2}F_l{}^-(5, x) + \tfrac{3}{4}F_l{}^-(3, x)\\
\mathrm{O}_l{}^{33}(x) &= \tfrac{25}{4}F_l{}^+(8, x) - \tfrac{15}{2}F_l{}^+(6, x) + \tfrac{9}{4}F_l{}^+(4, x)
\end{aligned}$$

and with

$$F_0{}^+(i, x) = \frac{2}{i-1} - Ei_i(Ax) - Ei_i(A(1-x))$$

$$F_1{}^+(i, x) = \frac{2x}{i-1} - Ei_i(A(1-x)) + \frac{1}{A}\left(Ei_{i+1}(Ax) - Ei_{i+1}(A(1-x))\right)$$

$$F_2{}^+(i, x) = \frac{2x^2}{i-1} + \frac{4}{A^2(i+1)} - Ei_i(A(1-x)) - \frac{2}{A}Ei_{i+1}(A(1-x)) - \frac{2}{A^2}\left(Ei_{i+2}(Ax) + Ei_{i+2}(A(1-x))\right)$$

$$F_0{}^-(i, x) = Ei_i(A(1-x)) - Ei_i(Ax)$$

$$F_1{}^-(i, x) = -\frac{2}{Ai} + Ei_i(A(1-x)) + \frac{1}{A}\left(Ei_{i+1}(Ax) + Ei_{i+1}(A(1-x))\right)$$

$$F_2{}^-(i, x) = -\frac{4x}{Ai} + Ei_i(A(1-x)) + \frac{2}{A}Ei_{i+1}(A(1-x)) + \frac{2}{A^2}\left(Ei_{i+2}(A(1-x)) - Ei_{i+2}(Ax)\right).$$

When these sources have been approximated by (12), the transmission probabilities are given by (15):

$$P_{Q_s,j^o}^{v\to i} = P_{0j^o}^{v\to i} + \sum_{m=1}^{M} \frac{S_m}{S_0} P_{mj^o}^{v\to i}$$

with

$$P_{0j}^{v\to i/o} = \frac{1}{Q} \sum_{l=0}^{L} a_l^0 G_{jl}^{\mp}$$

$$P_{1j}^{v\to i/o} = \frac{1}{Q} \sum_{l=0}^{L} a_l^1 G_{j+1,l}^{\mp}$$

$$P_{2j}^{v\to i/o} = \frac{1}{Q} \sum_{l=0}^{L} a_l^2 \left(\tfrac{3}{2} G_{j+2,l}^{\mp} - \tfrac{1}{2} G_{jl}^{\mp}\right)$$

$$P_{3j}^{v\to i/o} = \frac{1}{Q} \sum_{l=0}^{L} a_l^3 \left(\tfrac{5}{2} G_{j+3,l}^{\mp} - \tfrac{3}{2} G_{j+1,l}^{\mp}\right)$$

$$Q = 2A \sum_{l=0}^{L} \frac{a_l^0}{l+1}$$

$$G_{j0}^{-} = \frac{1}{j+2} - Ei_{j+3}(A) = G_{j0}^{+}$$

$$G_{j1}^{-} = -Ei_{j+3}(A) + \frac{1}{A}\left(\frac{1}{j+3} - Ei_{j+4}(A)\right)$$

$$G_{j1}^{+} = \frac{1}{j+2} - \frac{1}{A}\left(\frac{1}{j+3} - Ei_{j+4}(A)\right)$$

$$G_{j2}^{-} = -Ei_{j+3}(A) + \frac{2}{A}\left(-Ei_{j+4}(A) + \frac{1}{A}\left(\frac{1}{j+4} - Ei_{j+5}(A)\right)\right)$$

$$G_{j2}^{+} = \frac{1}{j+2} - \frac{2}{A}\left(\frac{1}{j+3} - \frac{1}{A}\left(\frac{1}{j+4} - Ei_{j+5}(A)\right)\right).$$